

Article

Synthesis and Spectroscopic Identification of Hybrid 3-(Triethoxysilyl)propylamine Phosphine Ruthenium(II) Complexes

Ismail Warad ^{1,*}, Saud Al-Resayes ¹, Zeid Al-Othman ¹, Salem S. Al-Deyab ² and El-Refaie Kenawy ²

¹ Department of Chemistry, King Saud University, P. O. Box 2455, Riyadh 11451, Saudi Arabia

² Petrochemical Research Chair, Department of Chemistry, King Saud University, P. O. Box 2455, Riyadh 11451, Saudi Arabia

* Author to whom correspondence should be addressed; E-Mail: warad@ksu.edu.sa;
Tel./Fax: +96-61-4675992.

Received: 21 April 2010; in revised form: 8 May 2010 / Accepted: 12 May 2010 /

Published: 17 May 2010

Abstract: An investigation into the potential ruthenium(II) **1-3** complexes of type $[\text{RuCl}_2(\text{P})_2(\text{N})_2]$ using triphenylphosphine and 1,3-*bis*-diphenylphosphinepropane and 3-(triethoxysilyl)propylamine has been carried out at room temperature in dichloromethane under an inert atmosphere. The structural behaviors of the phosphine ligands in the desired complexes during synthesis were monitored by $^{31}\text{P}\{^1\text{H}\}$ -NMR. The structure of complexes **1-3** described herein has been deduced from elemental analyses, infrared, FAB-MS and ^1H -, ^{13}C - and ^{31}P -NMR spectroscopy. Xerogels **X1-X3** were synthesized by simple sol-gel process of complexes **1-3** using tetraethoxysilane as co-condensation agent in methanol/THF/water solution. Due to their lack of solubility, the structures of **X1-X3** were determined by solid state ^{13}C -, ^{29}Si - and ^{31}P -NMR spectroscopy, infrared spectroscopy and EXAFS.

Keywords: Ru(II) complexes; phosphine; ether-phosphine; EXAF; Sol-gel; NMR

1. Introduction

Phosphines and diphosphines have been intensively used as monodentate and bidentate ligands in coordination chemistry because of their electron-donating power [1–10]. Metal complexes containing phosphorus ligands have always been important, due to their possible catalytic activity, and a variety of them have already been reported in literature [10–35]. In general diphosphine forms more stable complexes than non-chelating phosphine analogues under the harsh reaction conditions required for catalysis [5–30].

Ether-phosphine P~O ligands are designed to act as monodentate (P~O) as well as bidentate (P^O) donor ligands. Due to the hemilabile character of the ether-phosphine ligand, the oxygen donor is regarded as an intramolecular solvent impeding decomposition of the complex by protection of vacant coordination sites [16–24]. The weak ruthenium-oxygen bonds in bis(chelate)ruthenium(II) complexes of the type $\text{Cl}_2\text{Ru}(\text{P}^{\wedge}\text{O})_2$ are easily cleaved during the reaction with other incoming ligands such as amine or diamine [20–24]. By employing ether-phosphine ligands in the synthesis of ruthenium(II) complexes, the introduction of diamines is kinetically controlled and the formation of by-products can be avoided [17–22]. Diaminediphosphineruthenium(II) complexes with ether-phosphine and classical phosphine ligands were already successfully employed in the catalytic hydrogenation of unsaturated ketones with high diastereo- and enantioselectivity [14,15,21,25–28].

Exchange of triphenylphosphine (PPh_3) or 1,3-*bis*-diphenylphosphinepropane (dppp) ligands on ruthenium(II) complexes by diamine or amine ligands to produce new families of ruthenium(II)/phosphine/amine complexes is currently one of our lines of investigation [1,3,10]. Due to the presence of phosphine atoms in the backbone of the coordinated ligands, the reaction or fluxional behavior of such complexes can be easily monitored by $^{31}\text{P}\{^1\text{H}\}$ -NMR. Due to the sensitivity of the phosphorus atom to the chemical environment considerable efforts have been expended to study the structural and ligand exchange behavior in ruthenium(II) complexes containing ether-phosphines or diphosphine ligands by following the $^{31}\text{P}\{^1\text{H}\}$ -NMR chemical shift changes [1,3,17–24].

The immobilization of metal complexes enables the long-term use of expensive or toxic catalysts and provides a clean and straightforward separation of the product(s) [36]. Compared to organic polymers, inorganic material-immobilized catalysts possess some advantages [37]. For example, they prevent the intermolecular aggregation of the active species because of their rigid structures, they do not swell or dissolve in organic solvents, and often exhibit superior thermal and mechanical stability under the catalytic conditions.

A typical interphase is generated by simultaneous co-condensation of T-functionalized ligands with various alkoxysilanes [1]. By the introduction of triethoxysilyl function group into the amine ligands coordinate complexes, these complexes can be easily supported to a polysiloxane matrix by sol-gel process in order to immobilize catalysts [1,30–34].

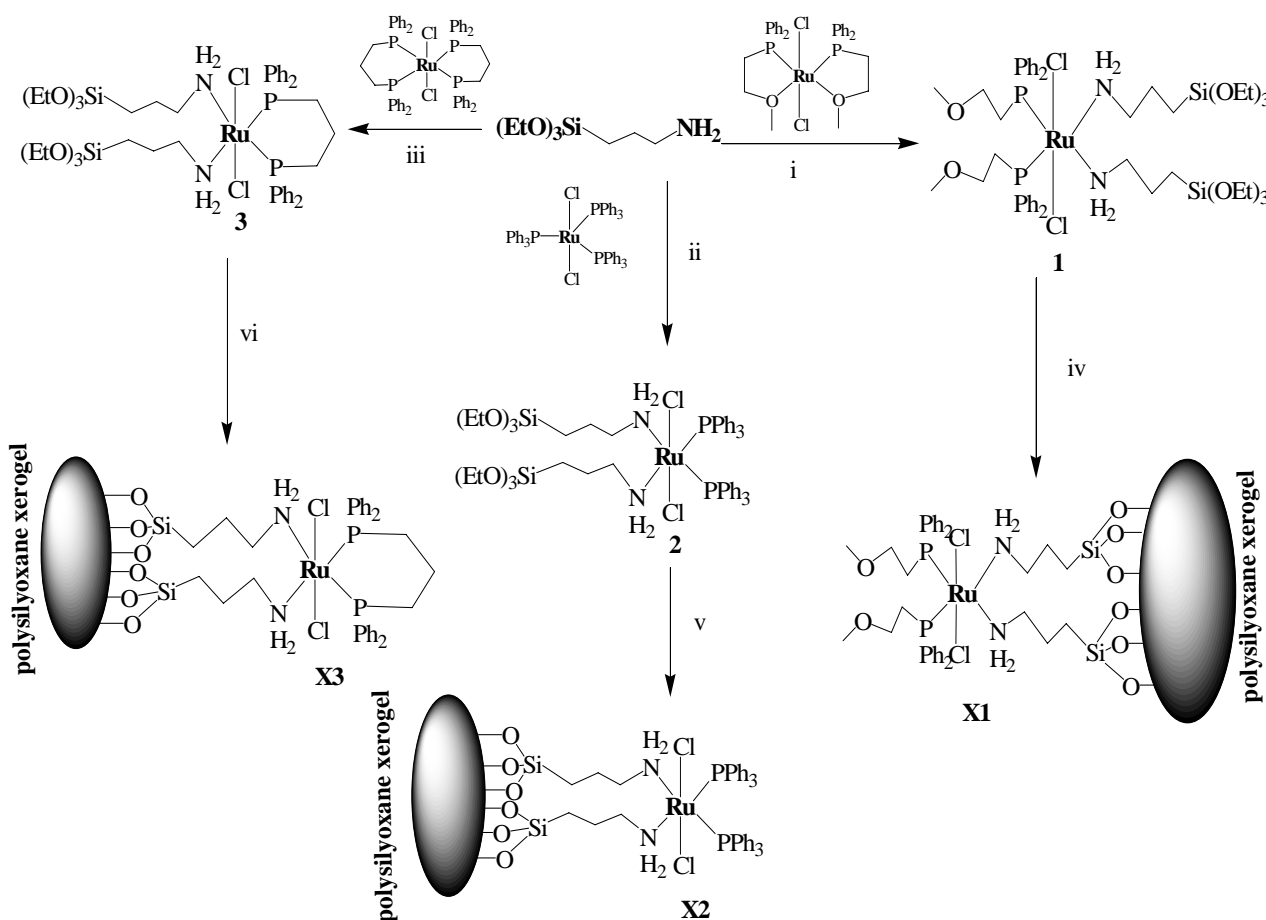
In this work a set of complexes of general formula $\text{RuCl}_2(\text{P})_2(\text{N})_2$ were prepared using monodentate phosphine and chelate diphosphine ligand in the presence of the monodentate 3-(triethoxysilyl)-propylamine co-ligand. The presence of $\text{Si}(\text{OEt})_3$ anchoring groups enabled the immobilization of the ruthenium(II) complexes through a simple sol-gel process using $\text{Si}(\text{OEt})_4$ as cross-linker.

2. Results and Discussion

2.1. Synthesis and ^{31}P -NMR investigation of ruthenium(II) complexes **1-3** and xerogels **X1-X3**

Three neutral Ru(II) complexes with PPh_3 , 2-(diphenylphosphino)ethyl methyl ether (etherphosphine, $\text{P}\sim\text{O}$), dppp ligands were coordinated with monodentate amine ligand in order to produce complexes of the $\text{trans-Cl}_2\text{Ru}(\text{P})_2(\text{N})_2$ type. Treating each of $\text{Cl}_2\text{Ru}(\text{P}^{\sim}\text{O})_2$, $\text{Cl}_2\text{Ru}(\text{PPh}_3)_3$ and $\text{Cl}_2\text{Ru}(\text{dppp})_2$ with two equivalent of 3-(triethoxysilyl)propylamine in dichloromethane resulted in the formation of complexes **1-3**, respectively, as shown in Scheme 1. Yellow powders with high melting points were obtained in very good yields. These complexes are soluble in chlorinated solvents such as chloroform, dichloromethane and insoluble in polar or non-polar solvents like water, methanol, diethyl ether and *n*-hexane.

Scheme 1. The synthetic route to prepare **1-3** complexes and **X1-X3** xerogels.

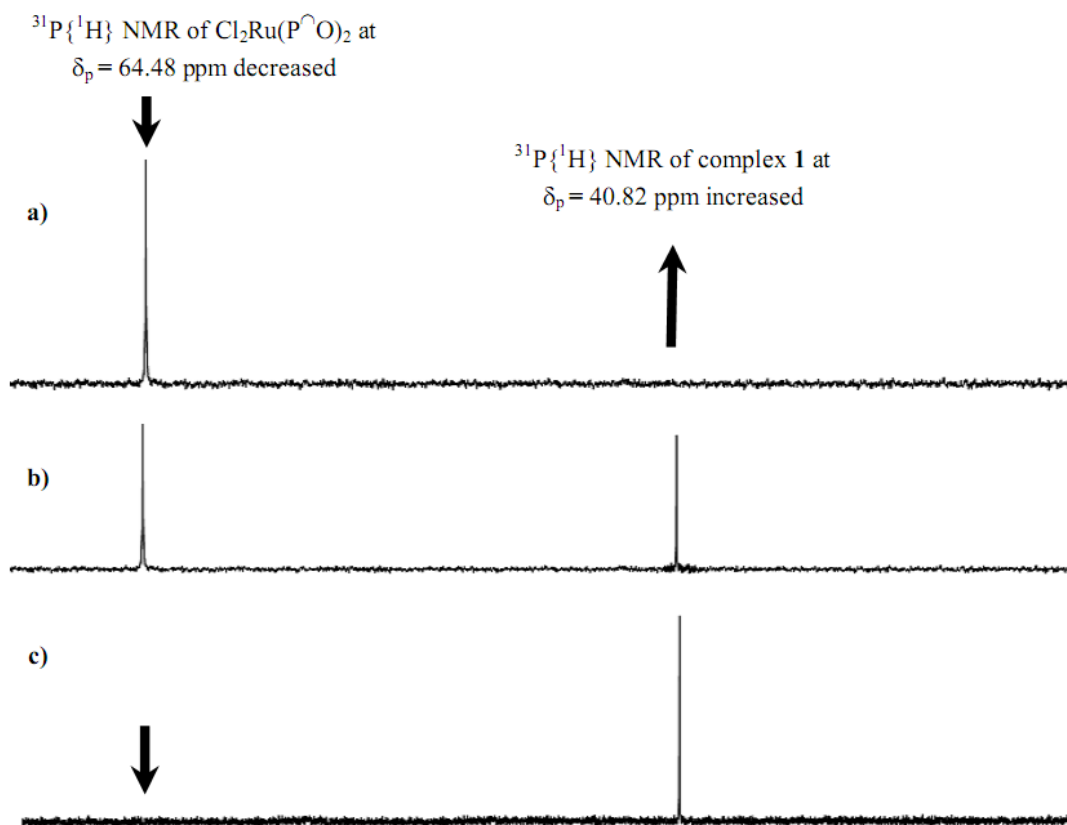


Reagents and conditions: i, ii, iii) CH_2Cl_2 , $25\text{ }^\circ\text{C}$, 5-60 min. stirring ;iv, v, vi) THF, H_2O , $\text{Si}(\text{OEt})_4$, $25\text{ }^\circ\text{C}$, 24 h stirring

Treating of $\text{Cl}_2\text{Ru}(\text{P}^{\sim}\text{O})_2$ with a slight excess of two equivalents of 3-(triethoxysilyl)propylamine in dichloromethane produced complex **1** as the $\text{trans-Cl}_2\text{Ru}(\text{P}\sim\text{O})_2(\text{NH}_2\text{R})_2$ isomer in very good yield. The stepwise formation was monitored by $^{31}\text{P}\{^1\text{H}\}$ spectroscopy, in the NMR tube experiment, addition of 3-(triethoxysilyl)propylamine to CDCl_3 solution containing $\text{Cl}_2\text{Ru}(\text{P}^{\sim}\text{O})_2$ generated a high field shift from $\delta_{\text{p}} = 64.4\text{ ppm}$ to $\delta_{\text{p}} = 40.8\text{ ppm}$.

The immediate disappearance of the complex $\text{Cl}_2\text{Ru}(\text{P}^{\wedge}\text{O})_2$ signal at $\delta_p = 64.4$ ppm upon 3-(triethoxysilyl)propylamine addition in parallel to the appearance of another signal at $\delta_p = 40.8$ ppm is related to formation of complex **1**, which was completed in two minutes without side product formation as shown in Figure 1.

Figure 1. Time-dependent $^{31}\text{P}\{^1\text{H}\}$ -NMR spectroscopic of $\text{Cl}_2\text{Ru}(\text{P}^{\wedge}\text{O})_2$ at $\delta_p = 64.4$ ppm mixed with two equivalent of 3-(triethoxysilyl)propylamine co-ligand in CDCl_3 in the NMR tube to produce complex **1** at $\delta_p = 40.8$ ppm a) before co-ligand addition, b) 1 min. and c) 2 min. after the co-ligand addition.



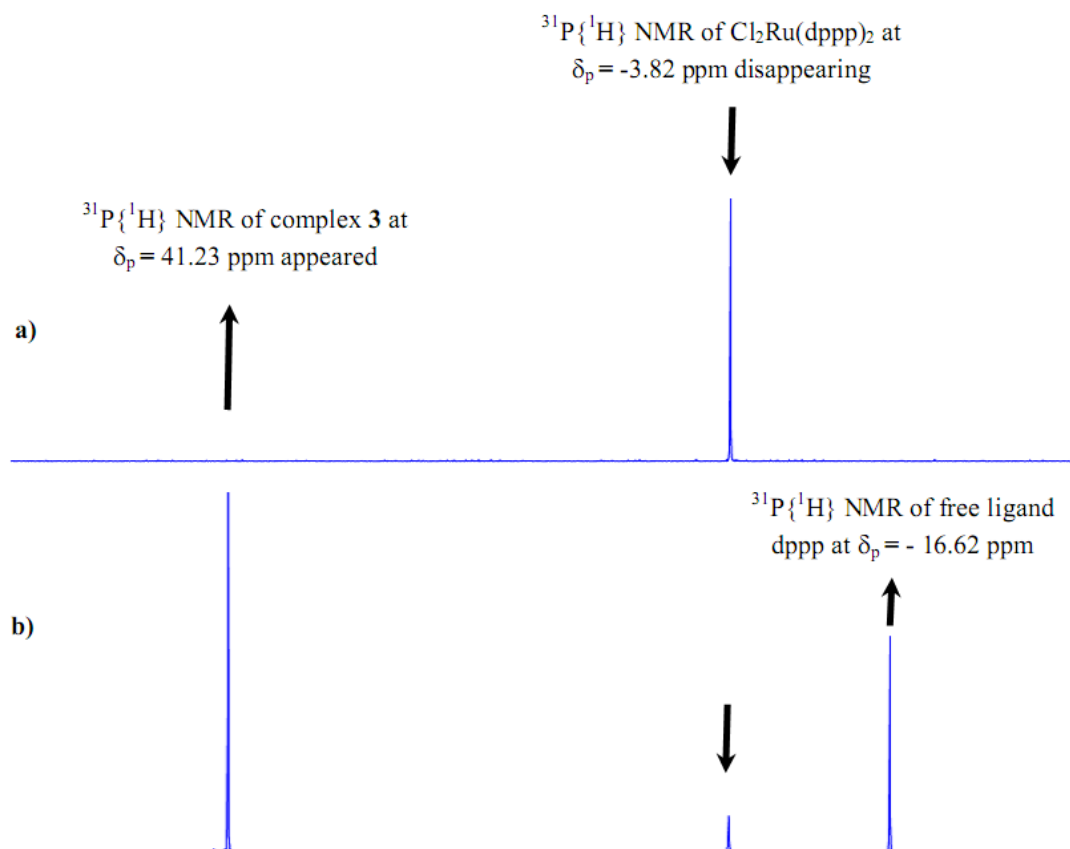
The two weak Ru-O bonds in $\text{Cl}_2\text{Ru}(\text{P}^{\wedge}\text{O})_2$ were cleaved by the two incoming molecules of the 3-(triethoxysilyl)propylamine co-ligand to form the two new Ru-N bonds of complex **1**. The presence of the hemilabile ether-phosphine ligand accelerated and stabilized such synthesis without any side products.

In the preparation of complex **2**, one molecule of PPh_3 ligand in $\text{Cl}_2\text{Ru}(\text{PPh}_3)_3$ was exchanged quantitatively by two equivalents of 3-(triethoxysilyl)propylamine in dichloromethane to form the most stable 18 electron valance shell complex **2** at $\delta_p = 45.8$ ppm as *trans*- $\text{Cl}_2\text{Ru}(\text{dppp})(\text{NH}_2\text{R})_2$ in good yield.

Complex **3** was obtained by a substitution reaction starting from $\text{Cl}_2\text{Ru}(\text{dppp})_2$ treated with 3-(triethoxysilyl)propylamine. Mixing of $\text{Cl}_2\text{Ru}(\text{dppp})_2$ with a slightly excess of two equivalents of 3-(triethoxysilyl)propylamine in dichloromethane enabled the preparation of complex **3** in a very good yield. The stepwise formation of complex **3** is easily monitored by $^{31}\text{P}\{^1\text{H}\}$ spectroscopy. Addition of 3-(trimethoxysilyl)propylamine in dichloromethane solution containing $\text{Cl}_2\text{Ru}(\text{dppp})_2$ generates a

downfield shift of ~ 45 ppm. One molecule of dppp ligand is exchanged rapidly by two molecules of the 3-(triethoxysilyl)propylamine co-ligands within 20 min to produce a complex of the *trans*- $\text{Cl}_2\text{Ru}(\text{dppp})(\text{NH}_2\text{R})_2$ type, traces of $\text{Cl}_2\text{Ru}(\text{dppp})_2$ at $\delta_{\text{p}} = -3.8$ ppm, in addition to the free dppp at $\delta_{\text{p}} = -16.6$ ppm and the product complex **3** at $\delta_{\text{p}} = 41.2$ ppm were recorded, as shown in Figure 2.

Figure 2. Time-dependent $^{31}\text{P}\{^1\text{H}\}$ -NMR spectroscopic of $\text{Cl}_2\text{Ru}(\text{dppp})_2$ at $\delta_{\text{p}} = -3.82$ ppm mixed with two equivalent of 3-(triethoxysilyl)propylamine co-ligand in dichloromethane to produce complex **3** at $\delta_{\text{p}} = 41.23$ ppm a) before ligand addition, b) 20 min. after ligand addition.



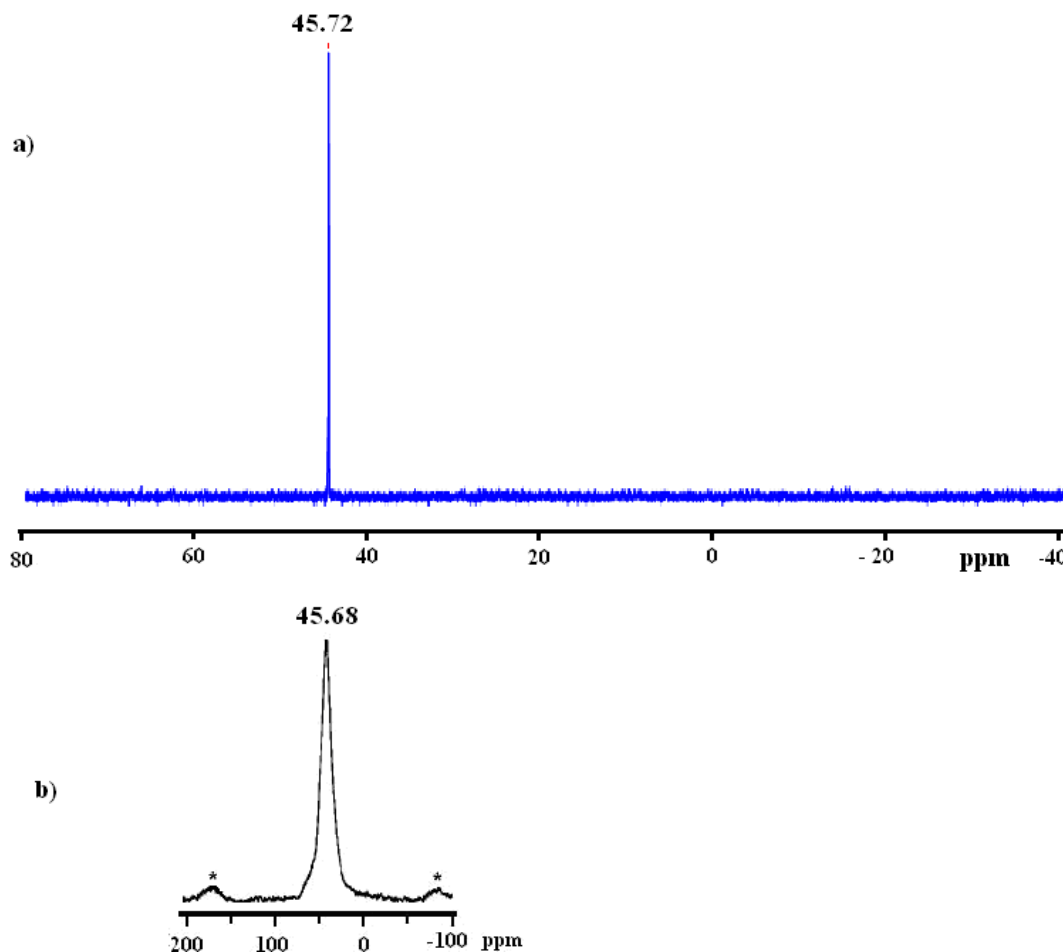
In these reactions, the combination of the change in the color from brown to light yellow and the $^{31}\text{P}\{^1\text{H}\}$ -NMR data confirmed the [1:2] diphosphine:amine fast-exchange reaction without any unexpected side reactions.

Compounds **1-3** were subjected to a sol-gel process with 10 equivalents of $\text{Si}(\text{OEt})_4$ using methanol/THF/water sol-gel conditions which allowed the preparation of non-soluble polysiloxane xerogels **X1-X3**, respectively. A typical sol-gel polymerization process at room temperature was carried out due to the presence of triethoxysilyl in the backbone of 3-(triethoxysilyl)propylamine ligand and $\text{Si}(\text{OEt})_4$. THF served as solvent for complexes **1-3**, while alcohol is necessary to homogenize the product and reactant mixture during the sol-gel process and water acts as initiator for the sol-gel process. Due to poor solubility of the **X1-X3** xerogels they were subjected to available solid state measurements like NMR, IR and EXAF.

Comparison of the solid state ^{31}P -MAS-NMR spectrum of the xerogel **X2** with the solution phase ^{31}P -NMR spectrum of complex **2** corroborated that no significant change of geometry in the

coordination sphere of the phosphorus atoms had taken place before or after the sol-gel process, as shown in Figure 3.

Figure 3. a) $^{31}\text{P}\{^1\text{H}\}$ of complex **2** in CD_2Cl_2 before sol-gel b) ^{31}P -CP/MAS-NMR spectrum of **X2** xerogel after sol-gel.

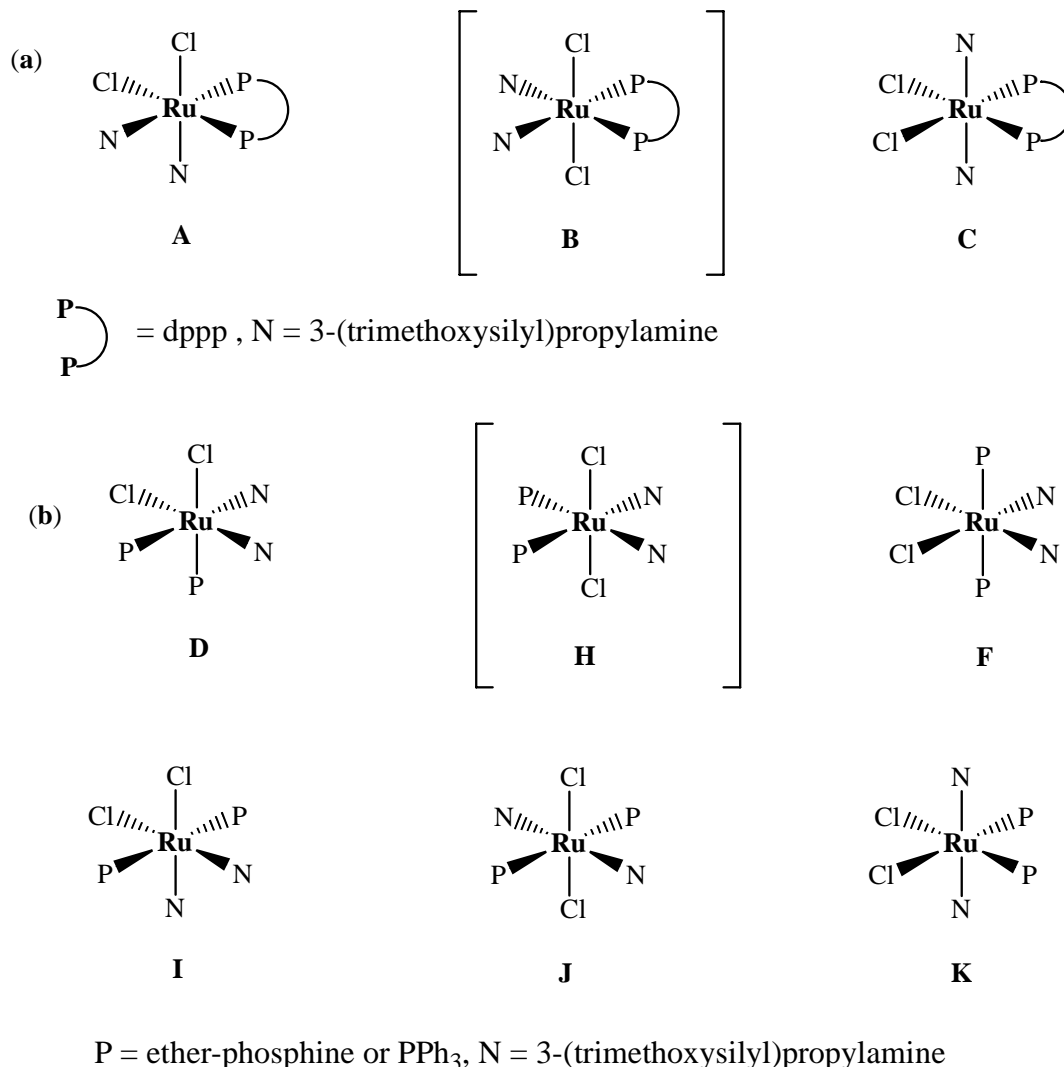


In the spectrum of the solid state material, side bands were observed due to the rotational frequency of the sample during measurements, and the peak was broader in comparison with the solution $^{31}\text{P}\{^1\text{H}\}$ -NMR result for complex **2**. Together the signals and the ^{31}P -NMR chemical shifts confirmed that the expected **2** and **X2** complexes were established with identical structure around the ruthenium(II) center atom.

Of interest is the use of $^{31}\text{P}\{^1\text{H}\}$ -NMR as a power tool to gain structural conformation about phosphorous-containing molecules and reaction processes. $^{31}\text{P}\{^1\text{H}\}$ -NMR chemical shifts, integrations, broadness and splitting can provide informative data about the favored isomers in the formation of $\text{RuCl}_2(\text{P})_2(\text{N})_2$ complexes.

In case where dppp was used to prepare complex **3**, the spectroscopic data are consistent with the coordination of these ligands in a static bidentate fashion which reduced the isomer number to three as in Scheme 2a, while the use of monodentate phosphine (PPh_3 or $\text{P}\sim\text{O}$) and amine ligands increased the isomer number to six, as in Scheme 2b.

Scheme 2. The possible geometries of: (a) three expected isomers of $\text{RuCl}_2(\text{PP})(\text{N})_2$ formula N-donor is monodentate amine ligands and PP-donor is bidentate phosphine ligand (dppp), (b) six expected isomers of $\text{RuCl}_2(\text{P})_2(\text{N})_2$ formula, where P-donor is monodentate phosphine ligands (PPh_3 or $\text{P}\sim\text{O}$).



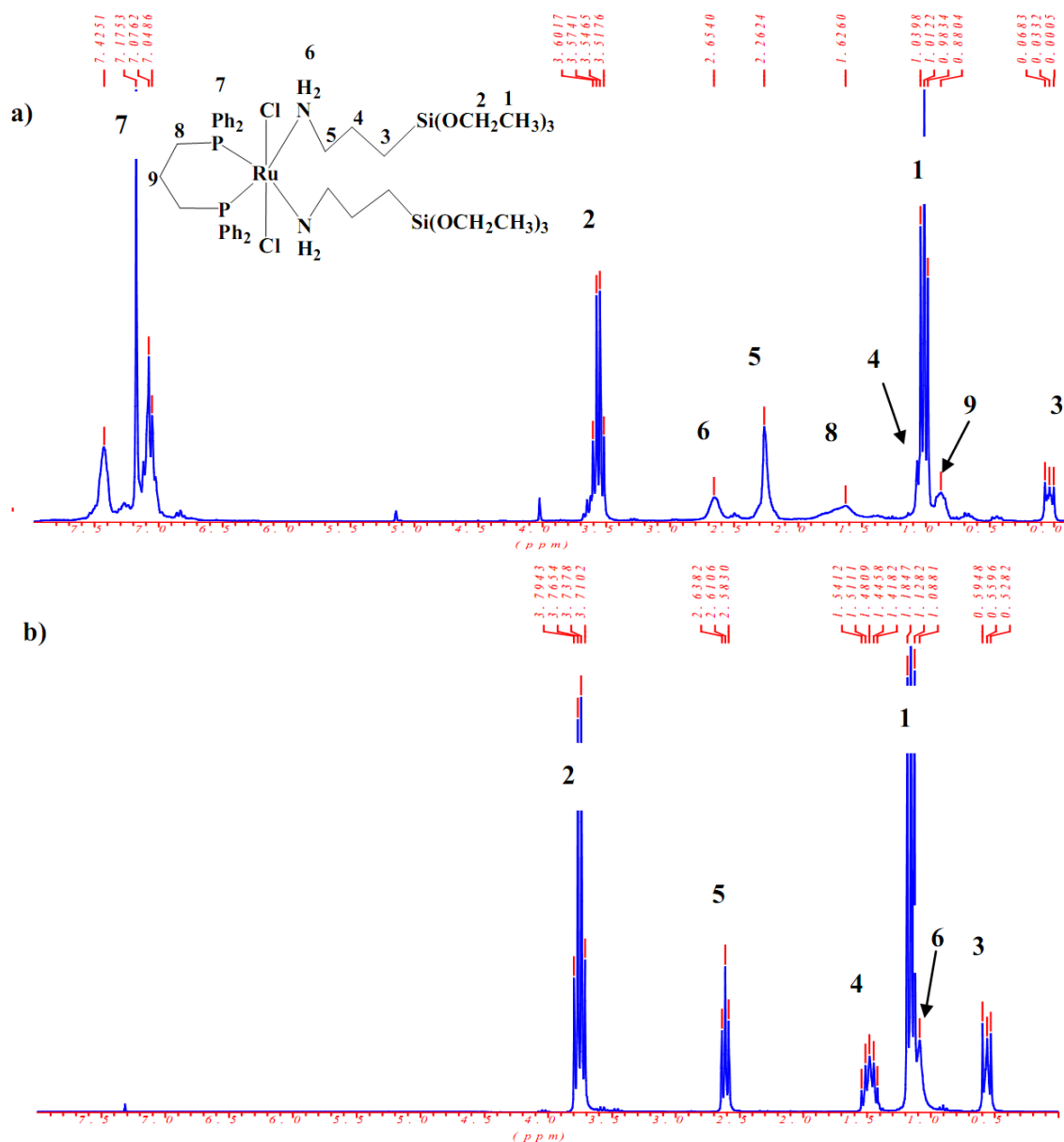
Due to the expected C_{2v} symmetry in such complexes, it is easily observed that all the above expected isomers **A-K** should show only sharp signals by P-NMR, except the thermodynamic isomers **A** and **D** which usually reveal an AB pattern P-NMR due to the unequivalent P split atoms in the backbone of the complexes (one P trans to N and the other trans Cl). Based on the $^{31}\text{P}\{^1\text{H}\}$ -NMR chemical shifts and our previous study on such complexes [1,2,10,17–24], it was anticipated that the kinetic favored isomers using both diphosphine and phosphine ligands of type **B** and **H** isomers (*trans*- RuCl_2 with nitrogen atoms are *trans* to phosphorus atoms) would be structurally favored over any other expected isomers [2,10,17–24]. The kinetically favored products *trans*- $[\text{RuCl}_2\text{P}_2\text{N}_2]$ isomer **B** and **H** were seen at $\delta_p \sim 40, 45, 41$ ppm for complexes **1-3** as well as **X1-X2** xerogels, respectively. No traces of the other non-favored isomers were detected by $^{31}\text{P}\{^1\text{H}\}$ -NMR at room temperature using dichloromethane or CDCl_3 as solvents.

2.2. H and C NMR investigations

In the ^1H -NMR spectra of the amine(phosphine)ruthenium(II) complexes **1-3** characteristic sets of signals were observed, which are attributed to the phosphine as well as 3-(triethoxysilyl)propylamine co-ligands. Their assignment was supported by the free ligand ^1H -NMR study. The integration of the ^1H resonances confirmed that the phosphines to amine ratios are in an agreement with the compositions of the desired complexes. As a typical example the ^1H -NMR of complex **3** was compared by the free 3-(triethoxysilyl)propylamine in Figure 4.

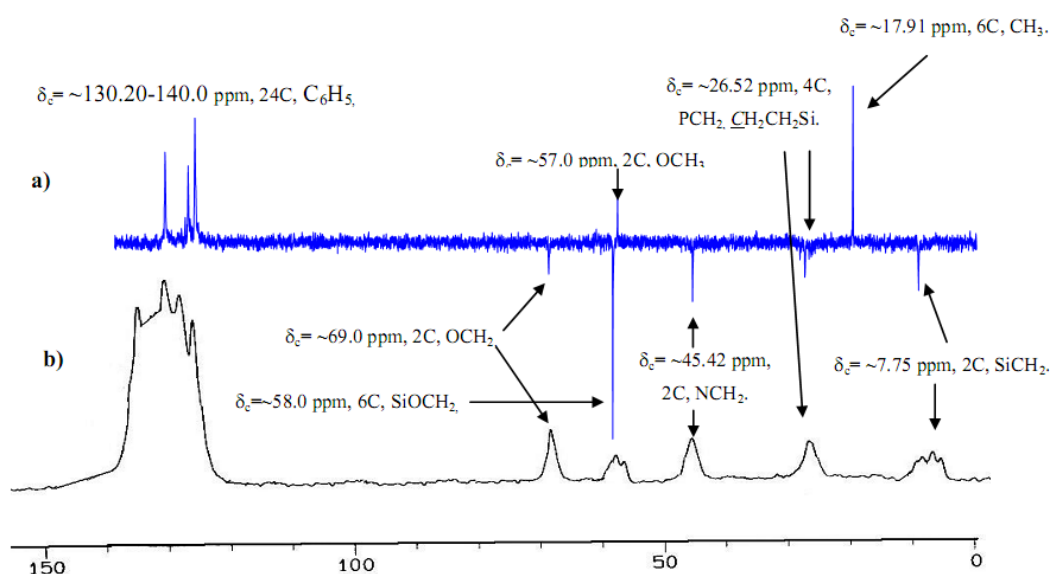
All the signals of 3-(triethoxysilyl)propylamine co-ligand in complex **3** are shifted to slightly higher field compared to the free ligands, except the H_2N protons which were moved to lower field from ~ 1 ppm to 2.6 ppm due to the direct coordination of the nitrogen atom to the ruthenium center. All other protons are in their expected regions, as shown in Figure 4.

Figure 4. ^1H -NMR of complex **3**: a) and free ligand 3-(triethoxysilyl)propylamine; b) in CDCl_3 at room temperature.



Characteristic sets of resonances phosphine as well as 3-(triethoxysilyl)propylamine are found in the $^{13}\text{C}\{^1\text{H}\}$ -NMR spectra of the desired complexes, which are attributed to the aliphatic part of the phosphine and diamine ligands, respectively. AXX' splitting patterns were observed for the aliphatic and aromatic carbon atoms directly attached to phosphorus. They are caused by the interaction of the magnetically inequivalent phosphorus atoms with the ^{13}C nuclei. This pattern is also consistent with isomers **B** and **H** (Scheme 2). Examination of the ^{13}C -CP-MAS-NMR spectrum of the modified solids along with the solution phase spectrum of the corresponding molecular precursor led to the conclusion that the organic fragments in **1** and **X1** remained intact during the grafting and subsequent workup without measurable decomposition (Figure 5).

Figure 5. $^1\text{Dept } 135$ ^{13}C -NMR of complex **1** in CDCl_3 a) compared by solid state ^{13}C -CP-MAS-NMR **X1** xerogels b).



The absence of CH_2O at $\delta_{\text{C}} = 50.8$ and CH_3 at $\delta_{\text{C}} = 18.2$ ppm belong to $(\text{CH}_3\text{CH}_2\text{O})_3\text{Si}$ of the 3-(triethoxysilyl)propylamine ligand after the sol-gel process of complex **1** to establish xerogel **X1**, were the major differences noted between spectra, which supported the immobilization of the desired hybrid Ru(II) complexes. The total disappearance of groups in **X1** (Figure 5b), compared by **1** (Figure 5a), provides good confirmation of a sol-gel process gone to full completion.

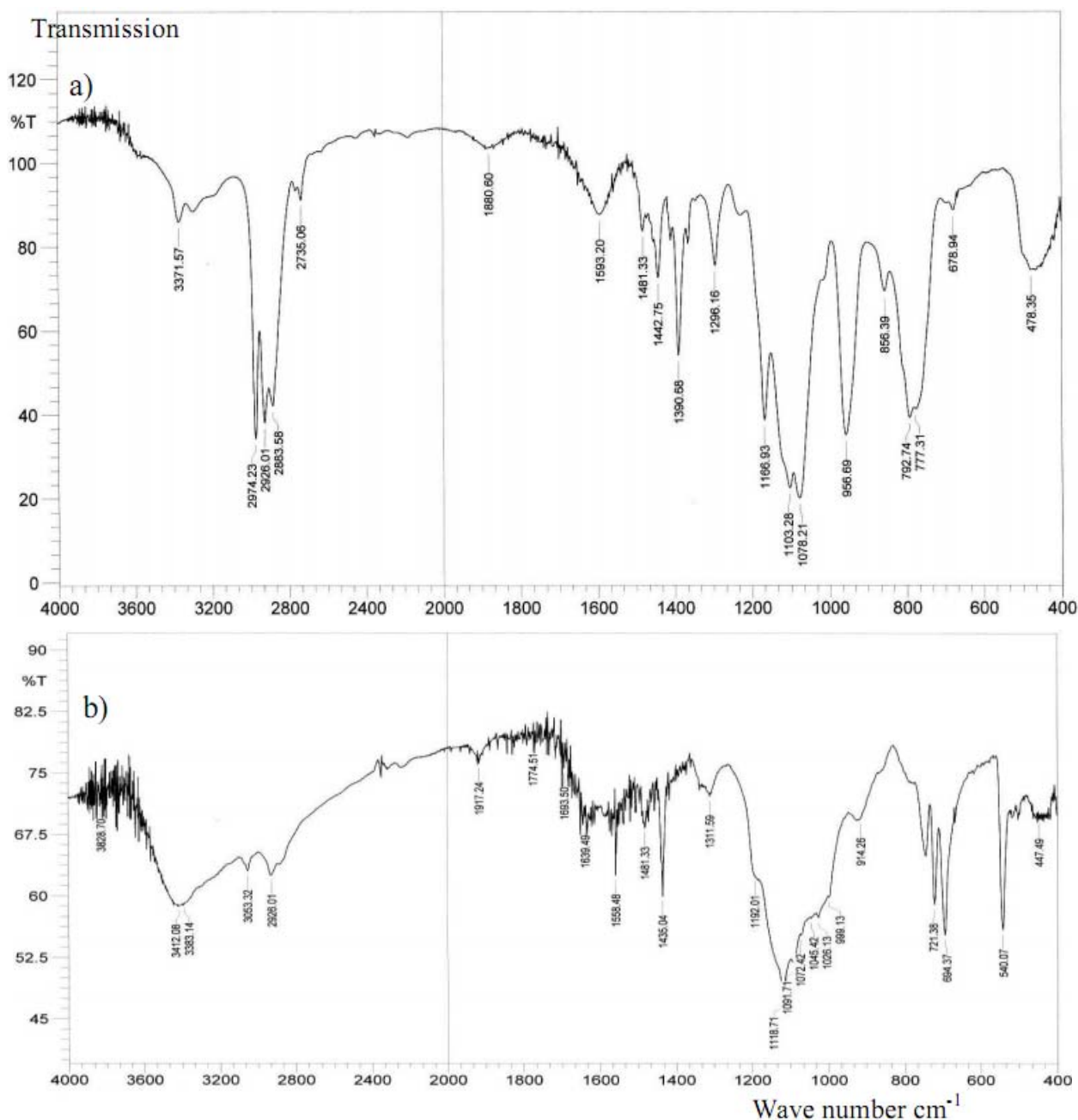
Solid-state ^{29}Si -NMR provided further information about the silicon environment and the degree of functionalization [1,30]. In all cases, the organometallic/organic fragment of the precursor molecule was covalently grafted onto the solid, and the precursors were, in general, attached to the surface of the polysiloxane by multiple siloxane bridges. The presence of T^{m} sites in case of xerogel **1-3** (with $m = 2$ and 3) in the spectral region of T^2 at $\delta_{\text{Si}} = -57.8$ ppm and T^3 at $\delta_{\text{Si}} = -67.1$ ppm as expected, Q^4 silicon sites due to $\text{Si}(\text{EtO})_4$ condensation agent were also recorded to Q^4 at $\delta_{\text{Si}} = -109.5$ ppm silicon sites of the silica framework.

2.3. IR investigations

In order to study the binding mode of the 3-(triethoxysilyl)propylamine and phosphine ligands to the ruthenium complexes and IR study was undertaken. The IR spectra of the desired complexes in

particular show several peaks which are attributed to stretching vibrations of the main functional groups in the $3,490\text{--}3,300\text{ cm}^{-1}$ (ν_{NH}), $3,280\text{--}3,010\text{ cm}^{-1}$ (ν_{PhH}) and $3,090\text{--}2,740\text{ cm}^{-1}$ (ν_{CH}) ranges. All other characteristic bands due to the other function groups are also present in the expected regions. To compare the structural vibration behaviors of these compounds against the infrared spectra of **3** and **X3** before and after the sol-gel processes are illustrated as typical examples in Figure 6.

Figure 6. Infra-red spectra (a and b) of **3** and **X3**, before and after sol-gel, respectively.

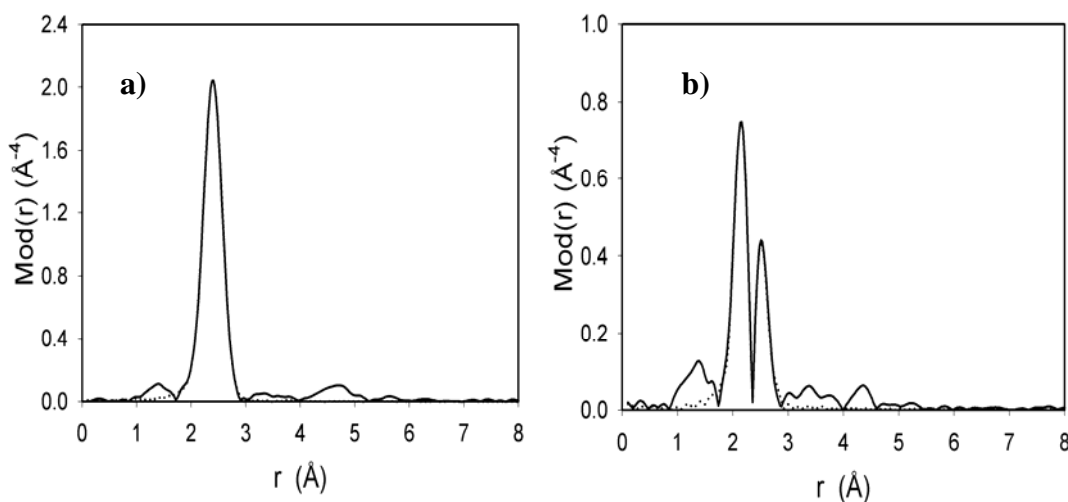


The broad intensive stretching vibrations at $2980\text{--}2840\text{ cm}^{-1}$ and bending vibration at $1000\text{--}950\text{ cm}^{-1}$ belonging to (ν_{CH}) of the $\text{SiOCH}_2\text{CH}_3$ function groups of complex **3** as in Figure 6a totally disappeared after the sol-gel process to prepare complex **X3** as seen in Figure 6b, which strongly confirms the completion of the sol-gel process formation.

2.4. EXAFS measurement of $\text{Cl}_2\text{Ru}(\text{dppp})_2$ complex and xerogel **X3**

EXAFS of starting material $\text{Cl}_2\text{Ru}(\text{dppp})_2$ complexes was measured before 3-(triethoxysilyl)propylamine addition then compared by EXAF of **X3** after sol-gel process of complex **3** to support the ligand exchange method of synthesis as well as to determine the bond lengths between the metal center and the coordinating atoms of the ligands.

Figure 7. Experimental (solid line) and theoretical (dotted line) Fourier Transform plot of $\text{Cl}_2\text{Ru}(\text{dppp})_2$ (a) and xerogel **X3** (b) measured at Ru K-edge.



The k^3 weighted EXAFS function of $\text{Cl}_2\text{Ru}(\text{dppp})_2$ can be best described by six different atom shells, four equivalent phosphorus and two chlorine atoms with Ru-P and Ru-Cl bond distances of 2.26 and 2.41 Å, are masked (due to the close in the bond lengths) in one relatively broad peak as in Figure 7a. The k^3 weighted EXAFS function of **X3** can also be described by six different atom shells. For the most intense peak of the Fourier Transform, two equivalent phosphorus, two nitrogen atoms and two chlorine atoms with Ru-P, Ru-N and Ru-Cl bond distances of 2.26, 2.19 and 2.41 Å, respectively, Ru-P and Ru-Cl bonds also masked in one peak but Ru-N bonds was appeared as an addition single peak compared with EXAF of $\text{Cl}_2\text{Ru}(\text{dppp})_2$ starting material as in Figure 7b, which strongly support the notion that one dppp ligand was exchanged by two 3-(triethoxysilyl)propylamine as well as no change around the ruthenium(II) between **3** and **X3** was detected due to the sol-gel immobilization.

3. Experimental

3.1. General remarks, materials, and instrumentation

All reactions were carried out in an inert atmosphere (argon) by using standard high vacuum and Schlenk-line techniques, unless otherwise noted. Prior to use CH_2Cl_2 , *n*-hexane, and Et_2O were distilled from CaH_2 , LiAlH_4 , and from sodium/benzophenone, respectively. 1,3-Bis(diphenylphosphino)propane (dppp), $\text{Cl}_2\text{Ru}(\text{P}^{\text{O}})_2$, $\text{Cl}_2\text{Ru}(\text{PPh}_3)_3$ and $\text{Cl}_2\text{Ru}(\text{dppp})_2$ were prepared according to literature methods [10,17]. 3-(Triethoxysilyl)propylamine was purchased from Acros. Elemental analyses were carried out on an Elementar Vario EL analyzer. High-resolution liquid ^1H -, $^{13}\text{C}\{^1\text{H}\}$ -,

DEPT 135, and $^{31}\text{P}\{^1\text{H}\}$ -NMR spectra were recorded on a Bruker DRX 250 spectrometer at 298 K. Frequencies are as follows: ^1H -NMR: 250.12 MHz, $^{13}\text{C}\{^1\text{H}\}$ -NMR: 62.9 MHz, and $^{31}\text{P}\{^1\text{H}\}$ -NMR 101.25 MHz. Chemical shifts in the ^1H - and $^{13}\text{C}\{^1\text{H}\}$ -NMR spectra were measured relative to partially deuterated solvent peaks which are reported relative to TMS. ^{31}P chemical shifts were measured relative to 85% H_3PO_4 . CP/MAS solid-state NMR spectra were recorded on Bruker DSX 200 (4.7 T) and Bruker ASX 300 (7.05 T) multinuclear spectrometers equipped with wide-bore magnets. Magic angle spinning was applied at 4 kHz (^{29}Si) and 10 kHz (^{13}C , ^{31}P) using (4 mm ZrO_2 rotors). Frequencies and standards: ^{31}P , 81.961 MHz (4.7 T), 121.442 MHz (7.05 T) [85% H_3PO_4 , $\text{NH}_4\text{H}_2\text{PO}_4$ ($\delta = 0.8$) as second standard]; ^{13}C , 50.228 MHz (4.7 T), 75.432 MHz (7.05 T) [TMS, carbonyl resonance of glycine ($\delta = 176.05$) as second standard]; ^{29}Si , 39.73 MHz (4.7 T), 59.595 MHz (7.05 T, (Q8M8 as second standard). All samples were prepared with exclusion of molecular oxygen. IR data were obtained on a Bruker IFS 48 FT-IR spectrometer. Mass spectra: EI-MS, Finnigan TSQ70 (200 °C) and FAB-MS, Finnigan 711A (8 kV), modified by AMD and reported as mass/charge (m/z). The EXAFS measurements were performed at the ruthenium K-edge (22118 eV) at the beam line X1.1 of the Hamburger Synchrotronstrahlungslabor (HASYLAB) at DESY Hamburg, under ambient conditions, energy 4.5 GeV, and initial beam current 120 mA. For harmonic rejection, the second crystal of the Si(311) double crystal monochromator was tilted to 30 %. Data were collected in transmission mode with the ion chambers flushed with argon. The energy was calibrated with a ruthenium metal foil of 20 μm thickness. The samples were prepared of a mixture of the samples and polyethylene.

3.2. General procedure for the preparation of the complex 1-3

3-(Triethoxysilyl)propylamine (0.10 g, 0.455 mmol, 5% excess) was dissolved in dichloromethane (5 mL) and the solution was added dropwise to a stirred solution of $\text{Cl}_2\text{Ru}(\text{P}^{\text{O}})_2$, $\text{Cl}_2\text{Ru}(\text{PPh}_3)_3$ or $\text{Cl}_2\text{Ru}(\text{dppp})_2$ (0.22 mmol) in dichloromethane (5 mL) within 2 min. The mixture was stirred for ca. 2 h at room temperature while the color changed from brown to yellow. Then the solution was concentrated to about 2 mL volume under reduced pressure. Addition of *n*-hexane (40 mL) caused precipitation of a yellow solid powder, which was filtered (P4). After recrystallization from dichloromethane/ diethyl ether, complexes **1-3** were obtained in analytically pure form in very good yields; m.p. > 340 °C (dec.).

Complex **1**: ^1H -NMR (CDCl_3): δ (ppm) 0.03 (m, 2H, CH_2Si), 1.08 (t, 18H, CH_3), 1.10 (m, 4H, SiCH_2CH_2), 1.48 (br, 4H, PCH_2), 2.06 (br, 4H, CH_2O), 2.31 (br, 4H, CH_2N), 2.55 (br, 4H, NH_2), 2.79 (s, 6H, OCH_3), 3.66 (m, 12H, OCH_2), 7.00–7.70 (m, 20H, C_6H_5); $^{31}\text{P}\{^1\text{H}\}$ -NMR (CDCl_3): δ (ppm) 40.82, s, $^{13}\text{C}\{^1\text{H}\}$ -NMR (CDCl_3): δ (ppm) 7.75 (s, 2C, CH_2Si), 17.91 (s, 6C, CH_3), 26.02 (m, 2C, PCH_2), 26.82 (s, 2C, $\text{CH}_2\text{CH}_2\text{Si}$), 45.42 (s, 2C, NCH_2), 57.93 (s, 2C, OCH_3), 58.71 (s, 6C, SiOCH_2), 69.39 (s, 2C, OCH_2) 127.20–134.0 (m, 24C, C_6H_5); FAB – MS; (m/z): 1102.3 (M^+); Anal. Calc. C, 52.26; H, 7.31; Cl, 6.43; N, 2.54 for $\text{C}_{48}\text{H}_{80}\text{Cl}_2\text{N}_2\text{O}_8\text{P}_2\text{RuSi}_2$: Found C, 52.44; H, 7.02; Cl, 6.43; N, 2.44%.

Complex **2**: $^1\text{H-NMR}$ (CDCl_3): δ (ppm) 0.05 (m, 2H, CH_2Si), 1.06 (t, 18H, CH_3), 1.11 (m, 4H, SiCH_2CH_2), 2.32 (br, 4H, CH_2N), 2.71 (br, 4H, NH_2), 3.61 (q, 12H, OCH_2), 7.10–7.80 (m, 30H, C_6H_5); $^{31}\text{P}\{^1\text{H}\}$ NMR (CDCl_3): δ (ppm) 45.7. s, $^{13}\text{C}\{^1\text{H}\}$ -NMR (CDCl_3): δ (ppm) 7.82 (s, 2C, CH_2Si), 17.21 (s, 6C, CH_3), 24.82 (s, 2C, $\underline{\text{C}}\text{H}_2\text{CH}_2\text{Si}$), 43.21 (s, 2C, NCH_2), 56.61 (s, 6C, OCH_2), 130.12–135.22 (m, 36C, C_6H_5); FAB-MS; (m/z): 1138.3 (M^+); Anal. Calc. C, 56.93; H, 6.72; Cl, 6.22; N, 2.46 for $\text{C}_{54}\text{H}_{76}\text{Cl}_2\text{N}_2\text{O}_6\text{P}_2\text{RuSi}_2$: Found C, 56.54; H, 6.42; Cl, 6.60; N, 2.35%.

Complex **3**: $^1\text{H-NMR}$ (CDCl_3): δ (ppm) 0.04 (m, 2H, CH_2Si), 0.88 (br, 2H, PCH_2CH_2), 1.01 (t, 18H, CH_3), 1.04 (m, 4H, SiCH_2CH_2), 1.82 (br, 4H, PCH_2CH_2), 2.26 (br, 4H, CH_2N), 2.65 (br, 4H, NH_2), 3.57 (q, 12H, OCH_2) 6.90–7.50 (m, 20H, C_6H_5); $^{31}\text{P}\{^1\text{H}\}$ -NMR (CDCl_3): δ (ppm) 41.73, s, $^{13}\text{C}\{^1\text{H}\}$ -NMR (CDCl_3): δ (ppm) 5.52 (s, 2C, CH_2Si), 16.61 (s, 6C, CH_3), 17.31 (s, 1C, $\text{PCH}_2\underline{\text{C}}\text{H}_2$), 24.22 (s, 2C, $\underline{\text{C}}\text{H}_2\text{CH}_2\text{Si}$), 24.82 (m, 2C, PCH_2), 43.21 (s, 2C, NCH_2), 56.61 (s, 6C, OCH_2), 126.09–132.82 (m, 24C, C_6H_5); FAB – MS; (m/z): 1026.2 (M^+); Anal. Calc. C, 52.62; H, 7.07; Cl, 6.90; N, 2.73 for $\text{C}_{45}\text{H}_{72}\text{Cl}_2\text{N}_2\text{O}_6\text{P}_2\text{RuSi}_2$: Found C, 52.34; H, 7.22; Cl, 6.70; N, 2.65%.

3.3. General procedure for sol–gel processing of xerogel **X1-X3**

Complexes **1-3** (0.100 mmol) and $\text{Si}(\text{OEt})_4$ (1 mmol, 10 equivalents) were mixed together in THF (5 mL). The sol–gel took place when a methanol/water mixture (2 mL, 1:1 v/v) was added to the solution. After 24 h stirring at room temperature, the precipitated gel was washed with toluene and diethyl ether (30 mL of each), and petroleum ether (20 mL). Finally the xerogel was ground and dried under vacuum for 24 h to afford after workup ~ 300 mg of a pale yellow powder were collected.

Xerogel X1: $^{31}\text{P-CP/MAS-NMR}$: $\delta = 40.9$ ppm; $^{13}\text{C-CP/MAS NMR}$: δ (ppm) 6.71 (m, 2C, CH_2Si), 27.22 (m, 4C, PCH_2 , $\underline{\text{C}}\text{H}_2\text{CH}_2\text{Si}$), 45.85 (br, 2C, NCH_2), 57.93 (m, 2C, OCH_3), 70.02 (br, 2C, OCH_2), 125.00–140.00 (m, 24C, C_6H_5); $^{29}\text{Si CP/MAS NMR}$: $\delta = -67.1$ ppm (T^3), -57.8 ppm (T^2), -109.5 ppm (Q^4).

Xerogel X2: $^{31}\text{P-CP/MAS-NMR}$: $\delta = 45.7$ ppm; $^{13}\text{C-CP/MAS NMR}$: δ (ppm): δ (ppm) 7.82 (m, 2C, CH_2Si), 24.82 (br, 2C, $\underline{\text{C}}\text{H}_2\text{CH}_2\text{Si}$), 45.21 (br, 2C, NCH_2), 130.12–140.22 (m, 36C, C_6H_5); CP/MAS NMR: $\delta = -67.1$ ppm (T^3), -57.8 ppm (T^2), -109.5 ppm (Q^4).

Xerogel X3: $^{31}\text{P-CP/MAS-NMR}$: $\delta = 41.7$ ppm; $^{13}\text{C-CP/MAS NMR}$: δ (ppm) 6.62 (m, 2C, CH_2Si), 17.31 (s, 1C, $\text{PCH}_2\underline{\text{C}}\text{H}_2$), 24.22 (s, 4C, $\underline{\text{C}}\text{H}_2\text{CH}_2\text{Si}$, PCH_2), 43.21 (s, 2C, NCH_2), 120.09–140.82 (m, 24C, C_6H_5); CP/MAS NMR: $\delta = -67.1$ ppm (T^3), -57.8 ppm (T^2), -109.5 ppm (Q^4).

4. Conclusions

Six ruthenium(II) complexes of the *trans*- $[\text{RuCl}_2(\text{P})_2(\text{N})_2]$ type were prepared using three types of phosphine ligands as well as 3-(triethoxysilyl)propylamine co-ligand. $^{31}\text{P}\{^1\text{H}\}$ -NMR was used to study the structural behavior of these complexes during the synthesis. The formation of the kinetically favored isomers of the desired complexes was confirmed by $^{31}\text{P-NMR}$. The presence of T-silyl functions on the amine co-ligand backbone in complexes **1-3** enables the hybridization of these

complexes in order to support them on a polysiloxane matrix through sol-gel processes using tetraethoxysilane as co-condensation agent in methanol/THF/water solution. The structure of complexes **1-3** described herein has been deduced from elemental analyses, infrared, FAB-MS and ^1H -, ^{13}C -, ^1H , and ^{31}P -NMR spectroscopy. Due to their lack of solubility, the structures of xerogels **X1-X3** were determined by solid state ^{13}C -, ^{29}Si - and ^{31}P -NMR spectroscopy, infrared spectroscopy and EXAFS.

Acknowledgements

The authors would like to thank Sabic Company for the financial support through project no. SCI-30-14, 2010.

References and Notes

1. Warad, I.; Al-Othman, Z.; Al-Resayes, S.; Al-Deyab, S.; Kenawy, E. Synthesis and characterization of novel inorganic-organic hybrid Ru(II) complexes and their application in selective hydrogenation. *Molecules* **2010**, *15*, 1028–1040.
2. Jakob, A.; Ecorchard, P.; Linseis, M.; Winter, R. Synthesis, solid state structure and spectro-electrochemistry of ferrocene-ethynyl phosphine and phosphine oxide transition metal complexes. *J. Organomet. Chem.* **2010**, *694*, 655–666.
3. Warad, I.; Siddiqui, M.; Al-Resayes, S.; Al-Warthan, A.; Mahfouz, R. Synthesis, characterization, crystal structure and chemical behavior of [1,1-bis(diphenylphosphinomethyl)ethene]ruthenium(II) complex toward primary alkylamine addition. *Trans. Met. Chem.* **2009**, *34*, 347–354.
4. Chang, C.-P.; Weng, C.-M.; Hong, F.-E. Preparation of cobalt sandwich diphosphine ligand $[(\eta^5\text{-C}_5\text{H}_4\text{Pr})\text{Co}(\eta^4\text{-C}_4(\text{PPh}_2)_2\text{Ph}_2)]$ and its chelated Palladium complex: Application of diphosphine ligand in the preparation of mono-substituted ferrocenylarenes. *Inorg. Chim. Acta* **2010**, *363*, 412–417.
5. Michelin, R.; Sgarbossa, P.; Scarso, A.; Strukul G. The Baeyer–Villiger oxidation of ketones: A paradigm for the role of soft Lewis acidity in homogeneous catalysis. *Coord. Chem. Rev.* **2010**, *254*, 646–660.
6. Wang, Z.-W.; Cao, Q.-Y.; Huang, X.; Lin, S.; Gao, X.-C. Synthesis, structure and electronic spectra of new three-coordinated Copper(I) complexes with tricyclohexylphosphine and diimine ligands. *Inorg. Chim. Acta* **2010**, *363*, 15–19.
7. James, B.; Lorenzini, F. Developments in the chemistry of tris(hydroxymethyl)phosphine. *Coord. Chem. Rev.* **2010**, *254*, 420–430.
8. Drozdak, R.; Allaert, B.; Ledoux, N.; Dragutan, I.; Dragutan, V.; Verpoort, F. Ruthenium complexes bearing bidentate Schiff base ligands as efficient catalysts for organic and polymer syntheses. *Coord. Chem. Rev.* **2005**, *249*, 3055–3074.
9. Tfouni, E.; Doro, F.; Gomes, A.; Silva, R.; Metzker, G.; Grac, P.; Benini, Z.; Franco, D. Immobilized ruthenium complexes and aspects of their reactivity. *Coord. Chem. Rev.* **2010**, *254*, 355–371.

10. Lindner, E.; Mayer, H. A.; Warad, I.; Eichele, K. Synthesis, characterization, and catalytic application of a new family of diamine(diphosphine)ruthenium(II) complexes. *J. Organomet. Chem.* **2003**, *665*, 176–185.
11. Xi, Z.; Hao, W.; Wang, P.; Cai, M. Ruthenium(III) chloride catalyzed acylation of alcohols, phenols, and thiols in room temperature ionic liquids. *Molecules* **2009**, *14*, 3528–3537.
12. Duraczynska, D.; Serwicka, E.M.; Drelinkiewicz, A.; Olejniczak, Z. Ruthenium(II) phosphine/mesoporous silica catalysts: The impact of active phase loading and active site density on catalytic activity in hydrogenation of phenylacetylene. *Appl. Catal. A. Gen.* **2009**, *371*, 166–172.
13. Premkumar, J.; Khoo, S. Immobilization of ruthenium(II)bipyridyl complex at highly oxidized glassy carbon electrodes. *Electrochem. Commun.* **2004**, *6*, 984–989.
14. Noyori, R. *Asymmetric Catalysis in Organic Synthesis*; Wiley and Sons: New York, NY, USA, 1994; pp. 16-46.
15. Noyori, R. Asymmetric Catalysis: Science and Opportunities. *Adv. Synth. Catal.* **2003**, *345*, 15–32 (Nobel Lecture).
16. Lindner, E.; Lu, Z.-L.; Mayer, A.H.; Speiser, B.; Tittel, C.; Warad, I. Cyclic voltammetric redox screening of homogeneous ruthenium(II) hydrogenation catalysts. *Electrochem. Commun.* **2005**, *7*, 1013–1020.
17. Lindner, E.; Warad, I.; Eichele, K.; Mayer, H.A. Synthesis and structures of an array of diamine(ether-phosphine)ruthenium(II) complexes and their application in the catalytic hydrogenation of *trans*-4-phenyl-3-butene-2-one. *Inorg. Chim. Acta* **2003**, *350*, 49–56.
18. Lu, Z.-L.; Eichele, K.; Warad, I.; Mayer, H.A.; Lindner, E.; Jiang, Z.; Schurig, V. Bis(methoxyethylmethylphosphine)ruthenium(II) complexes as transfer hydrogenation catalysts. *Z. Anorg. Allg. Chem.* **2003**, *629*, 1308–1315.
19. Warad, I.; Lindner, E.; Eichele, K.; Mayer, A.H. Cationic Diamine(ether-phosphine)ruthenium(II) complexes as precursors for the hydrogenation of *trans*-4-phenyl-3-butene-2-one. *Inorg. Chim. Acta* **2004**, *357*, 1847–1853.
20. Lindner, E.; Ghanem, A.; Warad, I.; Eichele, K.; Mayer, H.A.; Schurig, V. Asymmetric hydrogenation of an unsaturated ketone by diamine(ether-phosphine)ruthenium(II) complexes and lipase-catalyzed kinetic resolution: A consecutive approach. *Tetrahedron Asymmetry* **2003**, *14*, 1045–1050.
21. Lindner, E.; Al-Gharabli, S.; Warad, I.; Mayer, H.A.; Steinbrecher, S.; Plies, E.; Seiler, M.; Bertagnolli, H. Diaminediphosphineruthenium(II) interphase catalysts for the hydrogenation of α,β -unsaturated ketones. *Z. Anorg. Allg. Chem.* **2003**, *629*, 161–171.
22. Lu, Z.-L., Eichele, K., Warad, I., Mayer, H.A.E. Lindner, Jiang, Z., Schurig, V. Bis(methoxyethylmethylphosphine)ruthenium(II) complexes as transfer hydrogenation catalysts. *Z. Anorg. Allg. Chem.* **2003**, *629*, 1308–1315.
23. Warad, I.; Al-Resayes, S.; Eichele, E. Crystal structure of *trans*-dichloro-1,3-propanediamine-bis[(2-methoxyethyl)diphenylphosphine]ruthenium(II), $\text{RuCl}_2\text{-(C}_3\text{H}_{10}\text{N}_2\text{)(C}_{15}\text{H}_{17}\text{OP)}_2$. *Z. Kristallogr. NCS* **2006**, *221*, 275–277.
24. Warad, I. Synthesis and crystal structure of *cis*-dichloro-1,2-ethylenediamine-bis[1,4-(diphenylphosphino)butane]ruthenium(II) dichloromethane disolvate, $\text{RuCl}_2\text{(C}_2\text{H}_8\text{N}_2\text{)(C}_{28}\text{H}_{28}\text{P}_2\text{)-2CH}_2\text{Cl}_2$. *Z. Kristallogr. NCS* **2007**, *222*, 415–417.

25. Ohkuma, T.; Koizumi, M.; Muniz, K.; Hilt, G.; Kabuta, C.; Noyori, R. *Trans*-RuH(η^1 -BH₄)(binap)(1,2-diamine): A Catalyst for asymmetric hydrogenation of simple ketones under base-free conditions". *J. Am. Chem. Soc.* **2002**, *124*, 6508–6509 and reference there in.
26. Hashiguchi, S.; Fujii, A.; Haack, K.-J.; Matsumura, K.; Ikariya, T.; Noyori, R.; Kinetic resolution of racemic secondary alcohols by Ru(II)-catalyzed hydrogen transfer. *Angew. Chem. Int. Ed. Engl.* **1997**, *36*, 288–290.
27. Haack, K.-J.; Hashiguchi, S.; Fujii, A.; Ikariya, T.; Noyori, R. The catalyst precursor, catalyst, and intermediate in the Ru-II-promoted asymmetric hydrogen transfer between alcohols and ketones. *Angew. Chem. Int. Ed. Engl.* **1997**, *36*, 285–288.
28. Abdur-Rashid, K.; Faatz, M.; Lough, A.J.; Morris, H.R. Catalytic Cycle for the asymmetric hydrogenation of prochiral ketones to chiral alcohols: Direct hydride and proton transfer from chiral catalysts *trans*-Ru(H)₂(diphosphine)(diamine) to ketones and direct Addition of Dihydrogen to the Resulting Hydridoamido Complexes. *J. Am. Chem. Soc.* **2001**, *123*, 7473–7474 and reference their in.
29. Brunel, D.; Bellocq, N.; Sutra, P.; Cauvel, A.; Laspearas, M.; Moreau, P.; Renzo, F.; Galarneau, A.; Fajula, F. Transition-metal ligands bound onto the micelle-templated silica surface. *Coord. Chem. Rev.* **1998**, *178–180*, 1085–1108.
30. Lindner, E.; Salesch T.; Brugger S.; Steinbrecher S.; Plies, E.; Seiler; M., Bertagnolli H.; Mayer A.M. Accessibility studies of sol-gel processed phosphane-substituted iridium(I) complexes in the interphase. *Eur. J. Inorg. Chem.* **2002**, 1998–2006
31. Sayah, R.; Flochc, M.; Framery, E.; Dufaud, V. Immobilization of chiral cationic diphosphine rhodium complexes in nanopores of mesoporous silica and application in asymmetric hydrogenation. *J. Mol. Cat. A. Chem.* **2010**, *315*, 51–59.
32. Ohkuma, T.; Takeno, H.; Honda, Y.; Noyori, R. Asymmetric hydrogenation of ketones with polymer-bound BINAP diamine ruthenium catalysts. *Adv. Synth. Catal.* **2001**, *343*, 369–375.
33. Lu, Z.-L.; Lindner, E.; Mayer, H.A. Applications of sol-gel-processed interphase Catalysts. *Chem. Rev.* **2002**, *102*, 3543–3578.
34. Chai, L.T.; Wang, W.W.; Wang, Q.R.; Tao, Q.R. Asymmetric hydrogenation of aromatic ketones with MeO-PEG supported BIOHEP/DPEN ruthenium catalysts. *J. Mol. Cat. A* **2007**, *270*, 83–88.
35. Kang, C.; Huang, J.; He, W.; Zhang, F. Periodic mesoporous silica-immobilized palladium(II) complex as an effective and reusable catalyst for water-medium carbon–carbon coupling reactions. *J. Organomet. Chem.* **2010**, *695*, 120–127.
36. Bergbreiter, D. Using soluble polymers to recover catalysts and Ligands. *Chem. Rev.* **2002**, *102*, 3345–3384.
37. Song, C.; Lee, S. Supported chiral catalysts on inorganic materials. *Chem. Rev.* **2002**, *102*, 3495–3524.

Sample Availability: Samples of the compounds are available from the authors.